

Unsplit-Field Implementation of the Higher-Order PML using Z-Transform Method and D-B Formulation for Arbitrary Media

Naixing Feng¹, Jianxiong Li¹, and Xiaoming Zhao²

¹ School of Electronics and Information Engineering
Tianjin Polytechnic University, Tianjin, 300387, China
fengnaixing@gmail.com, lijianxiong@tjpu.edu.cn

² School of Textiles
Tianjin Polytechnic University, Tianjin, 300387, China
zhaoxiaoming@tjpu.edu.cn

Abstract — On the basis of the stretched coordinate perfectly matched layer (SC-PML) formulations, the Z-transform method, and D-B formulation, an efficient and unsplit-field implementation of the higher-order PML scheme with more than one pole is proposed to truncate the finite-difference time-domain (FDTD) lattices. This method is completely independent of the material properties of the FDTD computational domain and hence can be applied to the modeling of arbitrary media without any modification. The higher-order PML has the advantages of both the conventional PML and the complex frequency shifted PML (CFS-PML) in terms of absorbing performances. The proposed algorithm is validated through two numerical tests carried out in three dimensional and two dimensional domains. It is shown in the numerical tests that the proposed PML formulations with the higher-order scheme are efficient in terms of attenuating both the low-frequency propagating waves and evanescent waves and reducing late-time reflections, and also hold much better absorbing performances than the conventional SC-PML and the convolutional PML (CPML) with the CFS scheme.

Index Terms — finite-difference time-domain (FDTD), perfectly matched layer (PML), and Z-transform method.

I. INTRODUCTION

Since the introduction of the perfectly matched layer (PML) absorbing boundary condition (ABC) by Berenger [1], various modified PMLs have been presented to terminate the finite-difference time-domain (FDTD) lattices. With the advantage of simple implementation in the corners and the edges of the PML regions, the stretched coordinate PML (SC-PML) [2] was proposed through mapping Maxwell's equations into a complex stretched coordinate space. As original Berenger's PML, the SC-PML formulations in [2] were ineffective at absorbing the evanescent waves. Besides, the complex frequency shifted PML (CFS-PML) [3], implemented by simply shifting the frequency dependent pole off the real axis and into the negative-imaginary half of the complex plane, has drawn considerable attention due to the fact that this PML is efficient in attenuating the low-frequency evanescent waves and reducing late-time reflections [4]. In [4], the convolutional PML (CPML), based on the SC-PML formulations and the convolution theorem, was presented in detail to efficiently implement the CFS-PML. However, the CFS-PML would have a poor absorption of low-frequency propagating waves as shown in [5-7]. To overcome the limitations of both the conventional PML and the CFS-PML, the higher-order PML was proposed by Correia, which retains the advantages of both the CFS-PML and conventional PML in [7]. It has shown that the second-order PML is highly effective in absorbing

both evanescent and low-frequency propagating waves in both open-region and periodic problems in [8]. In [8], the 2nd-order PML based on the SC-PML was implemented by using the split-field PML formulations and the auxiliary differential equation (ADE) method. However, besides the drawback of more requirements of the memory and the computational time, the higher-order PML implementation proposed in [8] was difficult to be extended to the case with more than two poles because the polynomial expansion was employed.

In this paper, an efficient and unsplit-field implementation of the higher-order PML based on SC-PML formulations and the Z-transform method is proposed. For convenience, this PML is referred to here as the MZT PML. The proposed MZT PML algorithm is different from the proposed PML algorithm in [9] and [10-15], the proposed MZT PML algorithm is based on D-B formulations, and this method is fully independent of the material properties of the FDTD computational domain and hence can be applied to the modeling of arbitrary media without any modification. In addition, the proposed higher-order PML scheme requires less memory and computational time as compared with that in [8]. Only the 2nd-order case is described in this paper, but this approach is easy to be applied to any number of poles.

II. FORMULATION

In three-dimensional (3-D) SC-PML regions, the normalized frequency-domain modified Maxwell's curl equations can be written as,

$$j\omega\epsilon_r(\omega)\mathbf{E}(\omega)=c_0\nabla_s\times\mathbf{H}(\omega) \quad (1)$$

$$j\omega\mu_r(\omega)\mathbf{H}(\omega)=-c_0\nabla_s\times\mathbf{E}(\omega), \quad (2)$$

where c_0 is the speed of light in free space, $\epsilon_r(\omega)$ and $\mu_r(\omega)$ are, respectively, the relative permittivity and permeability of the FDTD computational domain and the operator ∇_s is expressed as,

$$\nabla_s = \hat{x}S_x^{-1}\partial_x + \hat{y}S_y^{-1}\partial_y + \hat{z}S_z^{-1}\partial_z \quad (3)$$

where ∂_x , ∂_y , and ∂_z are the partial derivatives with respect to x , y , and z and S_η , ($\eta = x, y, z$) are the complex stretched coordinate metrics, which was originally proposed [1] to be,

$$S_\eta = 1 + \sigma_\eta / j\omega\epsilon_0 \quad (4)$$

with the CFS scheme and S_η ($\eta = x, y, z$) were defined as,

$$S_\eta = \kappa_\eta + \sigma_\eta / (\alpha_\eta + j\omega\epsilon_0) \quad (5)$$

where σ_η and α_η are assumed to be positive real and κ_η is real and ≥ 1 . In order to make the PML completely independent of the material properties of the FDTD computational domain, both equations (1) and (2) can be written in terms of the electric flux density \mathbf{D} and the magnetic flux density \mathbf{B} as,

$$j\omega\mathbf{D}(\omega)=c_0\nabla_s\times\mathbf{H}(\omega) \quad (6)$$

$$j\omega\mathbf{B}(\omega)=-c_0\nabla_s\times\mathbf{E}(\omega), \quad (7)$$

where \mathbf{D} and \mathbf{B} are given by,

$$\mathbf{D}(\omega)=\epsilon_r(\omega)\mathbf{E}(\omega) \quad (8)$$

$$\mathbf{B}(\omega)=\mu_r(\omega)\mathbf{H}(\omega). \quad (9)$$

Consequently, this PML can be applied to truncate arbitrary media, such as lossy, dispersive, anisotropic, inhomogeneous or nonlinear without any modification and all that is needed is to modify equations (8) and (9) under consideration. The method is available in [16] to obtain \mathbf{E} from \mathbf{D} using equation (8) [and \mathbf{H} from \mathbf{B} using equation (9)]. It must be noted that if $\epsilon_r(\omega)$ or $\mu_r(\omega)$ is not frequency-dependent, \mathbf{E} or \mathbf{H} formulation should be adopted to reduce memory requirement and save computational time.

The idea of the higher-order PML was proposed in [8] by generalizing this metric for the case where more than one pole was present. For the 2nd-order PML, S_η is defined as,

$$S_\eta = S_{1\eta} \cdot S_{2\eta} = \left(\kappa_{1\eta} + \frac{\sigma_{1\eta}}{\alpha_{1\eta} + j\omega\epsilon_0} \right) \left(\kappa_{2\eta} + \frac{\sigma_{2\eta}}{\alpha_{2\eta} + j\omega\epsilon_0} \right). \quad (10)$$

Owing to the frequency dependence of S_η , the transformation of equation (6) to the time domain will lead to convolutions on the right hand side [4]. However, because the convolution in the time domain is just a multiplication in the Z-domain [17], it is more efficient as shown below that equation (6) is first transformed to the Z-domain and then to the FDTD form.

$$\frac{1-z^{-1}}{\Delta t}\epsilon_0 D_x = S_y(z) \cdot \frac{\partial H_z}{\partial y} - S_z(z) \cdot \frac{\partial H_y}{\partial z} \quad (11)$$

where Δt is the time step and $S_\eta(z)$, ($\eta = y, z$), is the z-transform of $1/S_\eta$, which can be obtained by first transforming $1/S_\eta$ to the s -domain using the relation $j\omega \rightarrow s$, and then applying the matched z -transform

method [17] using the relation $(s-p) \rightarrow (1-e^{p\Delta t}z^{-1})$,

$$S_\eta(z) = w_{1\eta} \left(\frac{1-h_{1\eta} \cdot z^{-1}}{1-g_{1\eta} \cdot z^{-1}} \right) \cdot w_{2\eta} \left(\frac{1-h_{2\eta} \cdot z^{-1}}{1-g_{2\eta} \cdot z^{-1}} \right) \quad (12)$$

where

$w_{m\eta} = 1/K_{m\eta}$, $g_{m\eta} = \exp[-(\Delta t/\varepsilon_0)(\alpha_{m\eta} + \sigma_{m\eta}/K_{m\eta})]$ and $h_{m\eta} = \exp(-\alpha_{m\eta}\Delta t/\varepsilon_0)$, ($m = 1, 2$). Substituting equation (12) into equation (11), we obtain

$$\begin{aligned} \frac{1-z^{-1}}{\Delta t} \varepsilon_0 D_x = \\ w_{1y} w_{2y} \left(\frac{1-h_{1y} \cdot z^{-1}}{1-g_{1y} \cdot z^{-1}} \right) \left(\frac{1-h_{2y} \cdot z^{-1}}{1-g_{2y} \cdot z^{-1}} \right) \frac{\partial H_z}{\partial y} \\ - w_{1z} w_{2z} \left(\frac{1-h_{1z} \cdot z^{-1}}{1-g_{1z} \cdot z^{-1}} \right) \left(\frac{1-h_{2z} \cdot z^{-1}}{1-g_{2z} \cdot z^{-1}} \right) \frac{\partial H_y}{\partial z}. \end{aligned} \quad (13)$$

Introducing four auxiliary variables Q_{xn} and P_{xn} ($\eta = y, z$).

$$\begin{aligned} Q_{xy} &= \frac{w_{1y} w_{2y} \Delta t}{\varepsilon_0} \cdot \left(\frac{1}{1-g_{1y} \cdot z^{-1}} \right) \cdot \frac{\partial H_z}{\partial y} \\ &= g_{1y} \cdot z^{-1} Q_{xy} + \frac{w_{1y} w_{2y} \Delta t}{\varepsilon_0} \cdot \frac{\partial H_z}{\partial y} \end{aligned} \quad (14)$$

$$\begin{aligned} P_{xy} &= \left(\frac{1-h_{2y} \cdot z^{-1}}{1-g_{2y} \cdot z^{-1}} \right) Q_{xy} \\ &= g_{2y} \cdot z^{-1} P_{xy} + Q_{xy} - h_{2y} \cdot z^{-1} Q_{xy}, \end{aligned} \quad (15)$$

$$\begin{aligned} Q_{xz} &= \frac{w_{1z} w_{2z} \Delta t}{\varepsilon_0} \cdot \left(\frac{1}{1-g_{1z} \cdot z^{-1}} \right) \cdot \frac{\partial H_y}{\partial z} \\ &= g_{1z} \cdot z^{-1} Q_{xz} + \frac{w_{1z} w_{2z} \Delta t}{\varepsilon_0} \cdot \frac{\partial H_y}{\partial z}, \end{aligned} \quad (16)$$

$$\begin{aligned} P_{xz} &= \left(\frac{1-h_{2z} \cdot z^{-1}}{1-g_{2z} \cdot z^{-1}} \right) Q_{xz} \\ &= g_{2z} \cdot z^{-1} P_{xz} + Q_{xz} - h_{2z} \cdot z^{-1} Q_{xz}. \end{aligned} \quad (17)$$

Considering that the z^{-1} operator corresponds to a single-step delay in the discrete time domain, equations (14) – (17) can be written in the FDTD form, respectively, as in equations (18) – (21), where

$$\begin{aligned} Q_{xy} \Big|_{i+1/2,j,k}^{n+1} &= g_{1y(j)} \cdot Q_{xy} \Big|_{i+1/2,j,k}^n \\ &+ u_{y(j)} \cdot \left(H_z \Big|_{i+1/2,j+1/2,k}^{n+1/2} - H_z \Big|_{i+1/2,j-1/2,k}^{n+1/2} \right) \end{aligned} \quad (18)$$

$$\begin{aligned} P_{xy} \Big|_{i+1/2,j,k}^{n+1} &= g_{2y(j)} \cdot P_{xy} \Big|_{i+1/2,j,k}^n \\ &+ Q_{xy} \Big|_{i+1/2,j,k}^{n+1} - h_{2y(j)} \cdot Q_{xy} \Big|_{i+1/2,j,k}^n, \end{aligned} \quad (19)$$

$$\begin{aligned} Q_{xz} \Big|_{i+1/2,j,k}^{n+1} &= g_{1z(k)} \cdot Q_{xz} \Big|_{i+1/2,j,k}^n \\ &+ u_{z(k)} \cdot \left(H_y \Big|_{i+1/2,j,k+1/2}^{n+1/2} - H_y \Big|_{i+1/2,j,k-1/2}^{n+1/2} \right), \end{aligned} \quad (20)$$

$$\begin{aligned} P_{xz} \Big|_{i+1/2,j,k}^{n+1} &= g_{2z(k)} \cdot P_{xz} \Big|_{i+1/2,j,k}^n \\ &+ Q_{xz} \Big|_{i+1/2,j,k}^{n+1} - h_{2z(k)} \cdot Q_{xz} \Big|_{i+1/2,j,k}^n. \end{aligned} \quad (21)$$

Equation (11) can be written as,

$$\begin{aligned} D_x \Big|_{i+1/2,j,k}^{n+1} &= D_x \Big|_{i+1/2,j,k}^n + P_{xy} \Big|_{i+1/2,j,k}^{n+1} - h_{1y(j)} \\ &\cdot P_{xy} \Big|_{i+1/2,j,k}^n - \left(P_{xz} \Big|_{i+1/2,j,k}^{n+1} - h_{1z(k)} \cdot P_{xz} \Big|_{i+1/2,j,k}^n \right) \end{aligned} \quad (22)$$

where $u_y = w_{1y} w_{2y} \Delta t / (\varepsilon_0 \Delta y)$, $u_z = w_{1z} w_{2z} \Delta t / (\varepsilon_0 \Delta z)$. Both Δy and Δz are the space steps. All coefficients, which are calculated once prior to the field computation and stored in one-dimensional vector arrays, auxiliary variables and field components, are evaluated at the corresponding Yee grid position. Noting that storage of $P_{xy} \Big|_{i+1/2,j,k}^n$, $P_{xz} \Big|_{i+1/2,j,k}^n$, $Q_{xy} \Big|_{i+1/2,j,k}^n$ and $Q_{xz} \Big|_{i+1/2,j,k}^n$ can be avoided by means of temporary storage variables [18]. Consequently, the FDTD implementation of equation (1) by using equations (18) – (22) requires only the storage of four auxiliary variables (i.e., P_{xy}^{n+1} , P_{xz}^{n+1} , Q_{xy}^{n+1} , and Q_{xz}^{n+1}) per field component per cell in the SC-PML region.

The above formulations are applied to the corner PML regions and the edge PML regions, which run parallel with x direction (i.e., both $S_y \neq 1$ and $S_z \neq 1$ are chosen as in equation (12)). In the faces of the PML regions, which are normal to the y direction and the edge PML regions that run parallel with the z direction (i.e., $S_y \neq 1$ as in equation (12) and $S_z = 1$ are chosen), E_x can be obtained by using only two auxiliary variables, P_{xy} and Q_{xy} . Likewise, in the faces of the PML regions, which are normal to the z direction and the edge PML regions that run parallel with the y direction (i.e., $S_y = 1$ and $S_z \neq 1$ as in equation (12) are chosen), E_x can be obtained by using only two auxiliary variables, P_{xz} and Q_{xz} . For the face PML regions, which are perpendicular to x direction (i.e., both $S_y = 1$ and $S_z = 1$ are chosen), no auxiliary variable is required. Similar formulations can be obtained for other field components of \mathbf{E} and \mathbf{H} .

In order to perform a comparison of the proposed formulations and the formulations in [8] in terms of memory, we assume a vacuum 3D FDTD computational domain with $L \times M \times N$ cells. A W -cell thick PML is used to truncate the FDTD computational domain on all directions. To obtain E_x , the proposed formulations require $4 \times (L+2W) \times W \times W \times 4 = 32W^3 + 16LW^2$ auxiliary variables in the corner PML regions and the edge PML regions, which run parallel with x direction (i.e., both $S_y \neq 1$ and $S_z \neq 1$ are chosen, and P_{xy} , P_{xz} , Q_{xy} , and Q_{xz} are required), $2 \times (L+2W) \times W \times N \times 2 = 8NW^2 + 4LNW$ auxiliary variables in the faces of the PML regions which are normal to y direction and the edge PML regions which run parallel with the z direction (i.e., $S_y \neq 1$ and $S_z = 1$ are chosen, and P_{xy} and Q_{xy} are required), $2 \times (L+2W) \times M \times W \times 2 = 8MW^2 + 4LMW$ auxiliary variables in the faces of the PML regions which are normal to the z direction and the edge PML regions that run parallel with the y direction (i.e., $S_y = 1$ and $S_z \neq 1$ are chosen, and P_{xz} and Q_{xz} are required), and 0 auxiliary variables in the face PML regions, which are perpendicular to the x direction (i.e., both $S_y = 1$ and $S_z = 1$ are chosen). By using the same means, auxiliary variables to obtain E_y , E_z , H_x , H_y , and H_z can be computed. In consequence, the proposed formulations require $192W^3 + 64(LW^2 + MW^2 + NW^2) + 16(LMW + LNW + MNW)$ auxiliary variables in total to obtain 6 field components. However, the formulations in [8] require $288W^3 + 112(LW^2 + MW^2 + NW^2) + 32(LMW + LNW + MNW)$ auxiliary variables. Therefore, the proposed formulations require $96W^3 + 48(LW^2 + MW^2 + NW^2) + 16(LMW + LNW + MNW)$ auxiliary variables less than the formulations in [8] in the PML regions.

As compared with [8], savings in the computation time can be achieved by the proposed algorithm due to the fact that the decrease of the auxiliary variables leads to the reduction of the calculation steps. The more the cells are required in the PML regions, the more the savings in memory and computation time. It is obvious that because of no polynomial expansion, the proposed implementation of the higher-order PML is easier than that in [8] to be extended to the case with more than two poles.

III. NUMERICAL RESULT

Two numerical tests are provided to validate the proposed method. In the first test, we implement the FDTD simulation for an inhomogeneous, dispersive, and conductive soil half-space problem in a highly elongated FDTD grid. It is shown in Fig. 1 that the dielectric constant of soil is specified as the second-order Debye model with an added term $\epsilon_r(\omega) = \epsilon_\infty + \sigma/j\omega\epsilon_0 + \sum_{p=1}^2 A_p/(1+j\omega\tau_p)$, where $\epsilon_\infty = 4.15$ is the infinite frequency permittivity, $A_1 = 1.8$ and $A_2 = 0.6$ are the pole amplitudes, $\tau_1 = 3.79$ nsec and $\tau_2 = 0.151$ nsec are the relaxation time and $\sigma = 1.11$ ms/m is the conductivity [19]. The half-space occupies 50 % of the vertical height of the horizontally elongated simulation region. The simulation is done with a $126 \times 46 \times 26$ grid including 10-cell-thick PML layers on all sides with the space steps $\Delta x = \Delta y = \Delta z = 0.05$ m and the time step $\Delta t = 77$ psec. Assuming that the origin is at a corner of FDTD grid, a vertically polarized point source located at (13, 13, 13) (just above the soil) is excited by a differentiated Gaussian pulse with a half pulse bandwidth = 1155 psec. Within the PML, σ_η and K_η are scaled using a fourth-order polynomial scaling [20] and α_η is a constant. The relative reflection error (in decibel) versus time is computed at an observation point located at (113, 33, 12) (at the opposing corner of FDTD grid from the source and just below the interface of free space and soil) by using,

$$R_{dB}(t) = 20 \log_{10} \left(\frac{|E_z(t) - E_{zref}(t)|}{|E_{zrefmax}|} \right) \quad (23)$$

where $E_z(t)$ represents the time-dependent discrete electric field of the observation point, $E_{zref}(t)$ is a reference solution based on a larger computational domain, and $E_{zrefmax}$ represents the maximum value of the reference solution over the full-time simulation. The relative reflection error is first computed over 1500 time iterations. This same example is repeated with SC-PML ($\alpha_\eta = 0$, $K_{max} = 11$, and $\sigma_{max} = 0.18$ S/m) and the convolutional PML (CPML) [4] ($\alpha_\eta = 0.0015$, $K_{max} = 7$, and $\sigma_{max} = 0.24$ S/m). For the 2nd-order PML including the formulations in [8] and the proposed formulations, the following parameters is chosen as follow, $K_{1\eta} = 1$, $\alpha_{1\eta} = 0$, $K_{2\eta opt} = 8$, $\sigma_{1\eta} = \sigma_{1\eta opt} \rho^4$, $K_{2\eta} = 1 + K_{2\eta opt} \rho^2$, $\sigma_{1\eta opt} = 0.175/150\pi\Delta x$, $\alpha_{2\eta} = 0.0015 + \sigma_{1\eta}$, $\sigma_{2\eta opt} = 4/150\pi\Delta x$ and $\sigma_{2\eta} = \sigma_{2\eta opt} \rho^2$ where ρ is

zero at the interface of the PML and the FDTD computational domains and 1 at the end. In all computations of this paper, σ and K are evaluated as the average value in the cell around the index location [1]. These optimum parameters are chosen empirically to obtain the lowest reflection. The difference of the optimum parameters of MZT PML and CPML results from different scheme (i.e., the coefficients of equations (18) – (22) are different from the counterpart of CPML).

These results are illustrated in Fig. 2. The maximum relative reflection errors of the conventional SC-PML, the CPML, the 2nd-order PML in [8] and the proposed 2nd-order PML are -43 dB, -52 dB, -68 dB, and -66 dB, respectively. It can be concluded from Fig. 2 that the absorbing performance of the proposed 2nd-order PML formulations have 14 dB and 23 dB improvement in terms of the maximum relative error as compared with the CPML and the SC-PML, respectively, and holds much lower reflection error for the late-time region than the CPML and the SC-PML.

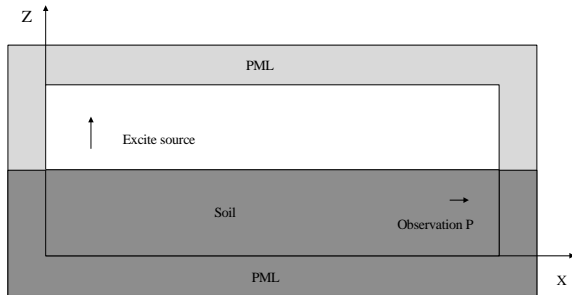


Fig. 1. 3D FDTD grid for an inhomogeneous, dispersive, and conductive soil half-space problem.

Tables 1 and 2 are using different perfectly matched layer algorithm procedures, which occupy memory and with different time steps occupy computational time, respectively. Obviously, when FDTD computational domain is invariant, saving memory will increase with the increase of PML layers and saving time will increase with the increase of time steps.

In the second test, to simplify the problem, but without loss of generality, we model a 2D TE-polarized electromagnetic wave interaction with an infinitely long perfectly electric conductor (PEC) sheet with the finite width to validate the proposed formulations. Figure 3 shows the FDTD

grid geometry used in this simulation. The space is discretized with the FDTD lattice with $\Delta x = \Delta y = 1$ mm and time step $\Delta t = 1.1785$ psec. The FDTD computational domains consist of a 100-cell wide PEC sheet surrounded by free space. 10-cell thick PML layers terminate the grid and are placed only 3-cells away from the PEC sheet in all directions.

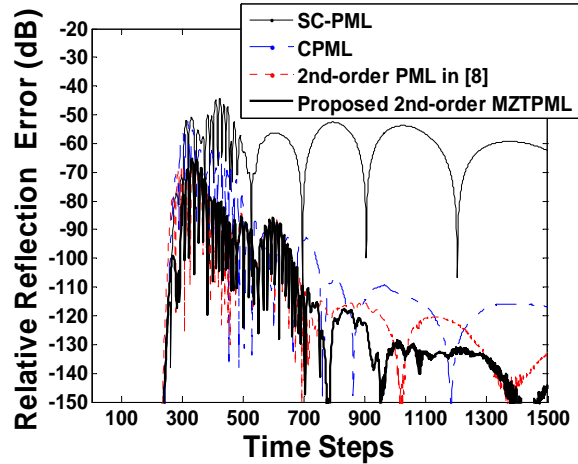


Fig. 2. Relative reflection error versus time, for the conventional SC-PML, CPML, 2nd-order PML in [8], and 2nd-order MZTPML.

Table 1: Using different perfectly matched layer algorithm procedures which occupy memory (bytes).

	PML layers=10	PML layers=16
2 nd -order PML in [8]	49,506K	105,509K
2 nd -order MZT PML	29,848K	65,224K
CPML	24,084K	49,664K
SC-PML	24,084K	49,672K

Table 2: Different time steps occupy computational time (s) (PML layers = 10).

	Time steps =2000	Time steps =4000
2 nd -order PML in [8]	667.60	1344.58
2 nd -order MZT PML	382.33	770.39
CPML	285.84	579.85
SC-PML	303.62	604.23

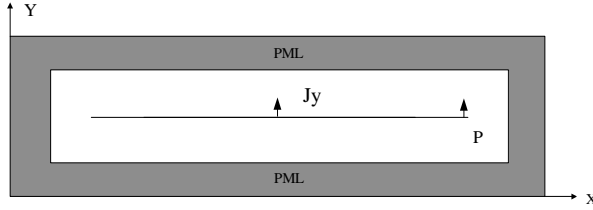


Fig. 3. The FDTD grid geometry in this simulation.

A y -polarized line electric current source, infinitely long in the z direction, is placed at the center and excited with a differentiated Gaussian pulse given by,

$$J_y(t) = -2 \frac{t-t_0}{t_w} \exp \left[-\left(\frac{t-t_0}{t_w} \right)^2 \right] \quad (24)$$

where $t_w = 26.53$ psec. and $t_0 = 4t_w$. The y -component of the electric field is measured at the point P , where we expect very strong evanescent waves to appear. The relative reflection error (in dB) versus time is computed at the observation point P by using,

$$R_{dB}(t) = 20 \log_{10} \left(\frac{|E_y^R(t) - E_y^T(t)|}{|E_{y_max}^R|} \right) \quad (25)$$

where $E_y^T(t)$ represents the time-dependent discrete electric field of the observation point, $E_y^R(t)$ is a reference solution based on a larger computational domain, and $E_{y_max}^R$ represents the maximum value of the reference solution over the full time simulation. The reference grid is sufficiently large such that there are no reflections from its outer boundaries during 1500 time steps, which are well past the steady-state response. The same example is repeated with the conventional SC-PML (equivalent to the CPML with $\alpha_\eta = 0$), the CPML and the 2nd-order PML in [8]. Within the conventional SC-PML and the CPML, K_η and σ_η are scaled by using a fourth-order polynomial scaling ($m = 4$) and α_η is a constant, as in [4]. The σ_{opt} is chosen as,

$$\sigma_{opt} = \frac{m+1}{150\pi\Delta x}.$$

For the conventional SC-PML, $K_{max} = 9$ and $\sigma_{max} = 0.5 \sigma_{opt}$ are chosen. In the CPML simulation, $K_{max} = 9$, $\sigma_{max} = 0.9 \sigma_{opt}$ and $\alpha_\eta = 0.06$ are chosen. For the 2nd-order PML including the formulations in [8] and

the proposed formulations, the following parameters are chosen, $K_{1\eta} = 1$, $\alpha_{1\eta} = 0$, $K_{2\eta_{opt}} = 8$, $\sigma_{1\eta} = \sigma_{1\eta_{opt}} \rho^4$, $K_{2\eta} = 1 + K_{2\eta_{opt}} \rho^2$, $\sigma_{1\eta_{opt}} = 0.075/150\pi\Delta x$, $\alpha_{2\eta} = 0.09 + \sigma_{1\eta}$, $\sigma_{2\eta_{opt}} = 4/150\pi\Delta x$ and $\sigma_{2\eta} = \sigma_{2\eta_{opt}} \rho^2$. These optimum parameters are chosen empirically to obtain the lowest reflection.

The results are illustrated in Fig. 4. The maximum relative errors of the conventional SC-PML, CPML, 2nd-order PML in [8] and MZT PML are -49 dB, -75 dB, -90 dB and -90 dB, respectively. It can be concluded from figure that the absorbing performance of the proposed 2nd-order PML formulations is similar to that in [8] and has 15 dB and 41 dB improvement in terms of the maximum relative error as compared with the CPML and the SC-PML, respectively.

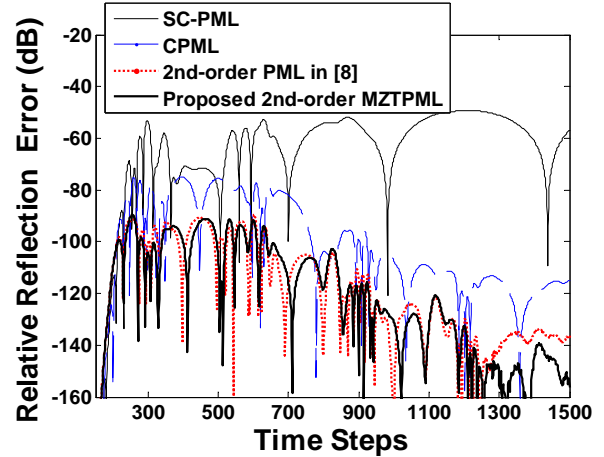


Fig. 4. Relative reflection error versus time for the conventional SC-PML, CPML, 2nd-order PML in [8], and 2nd-order MZT PML.

Tables 3 and 4 are similar to the first test by using different perfectly matched layer algorithm procedures which occupy of memory and different time steps that occupy computational time, respectively. Obviously, when FDTD computational domain is invariant, saving memory will increase with the increase of PML layers and saving time will increase with the increase of time steps.

IV. CONCLUSION

An efficient and unsplit-field implementation of the higher-order PML based on the SC-PML and

the z -transform method has been presented. It can be shown in the numerical tests that the proposed 2nd-order PML formulations hold better absorbing performance in terms of attenuating both the low-frequency propagating waves and evanescent waves and require less memory and computational time compared with the 2nd-order PML formulations implemented by using the split-field PML formulations and the auxiliary differential equation (ADE) method.

Table 3: Using different perfectly matched layer algorithm procedures, which occupy memory (bytes).

	PML layers=10	PML layers=16
2 nd -order PML in [8]	1,256K	1,500K
2 nd -order MZT PML	1,204K	1,412K
CPML	1,196K	1,220K
SC-PML	1,332K	1,428K

Table 4: Different time steps occupy computational time (s) (PML layers =10).

	Time steps =60000	Time steps =90000
2 nd -order PML in [8]	61.60	92.46
2 nd -order MZT PML	57.47	86.70
CPML	54.49	81.89
SC-PML	66.75	100.57

ACKNOWLEDGMENT

This work is supported by the Research Project of Applied Basic and Front Technologies of Tianjin (Grant No. 10JCZDJC15400) and the Natural Science Foundation of Tianjin (Grant No. 11JCYBJC26400).

REFERENCES

- [1] J. P. Bérenger, "A perfectly matched layer for the absorption of electromagnetic waves," *J. Computat. Phys.*, vol. 114, no. 2, pp. 185-200, Oct. 1994.
- [2] W. C. Chew and W. H. Weedon, "A 3-D perfectly matched medium from modified Maxwell's

equations with stretched coordinates," *Microw. Opt. Technol. Lett.*, vol. 7, no. 13, pp. 599-603, Sep. 1994.

- [3] M. Kuzuoglu and R. Mittra, "Frequency dependence of the constitutive parameters of causal perfectly matched anisotropic absorbers," *IEEE Microw. Guided Wave Lett.*, vol. 6, no. 12, pp. 447-449, Dec. 1996.
- [4] J. A. Roden and S. D. Gedney, "Convolution PML (CPML): An efficient FDTD implementation of the CFS-PML for arbitrary media," *Microw. Opt. Technol. Lett.*, vol. 27, no. 5, pp. 334-339, Dec. 2000.
- [5] E. Bécache, P. G. Petropoulos, and S. D. Gedney, "On the long-time behavior of unsplit perfectly matched layers," *IEEE Trans. Antennas Propag.*, vol. 52, no. 5, pp. 1335-1342, May 2004.
- [6] J. P. Bérenger, "Numerical reflection from FDTD-PMLs: a comparison of the split PML with the unsplit CFS PML," *IEEE Trans. Antennas Propag.*, vol. 50, no. 3, pp. 258-265, Mar. 2002.
- [7] D. Correia and J. M. Jin, "Performance of regular PML, CFS-PML, and second-order PML for waveguide problems," *Microw. Opt. Technol. Lett.*, vol. 48, no. 10, pp. 2121-2126, Oct. 2006.
- [8] D. Correia and J. M. Jin, "On the development of a higher-order PML," *IEEE Trans. Antennas Propag.*, vol. 53, no. 12, pp. 4157-4163, Dec. 2005.
- [9] N. Feng and J. Li "A Z-transform implementation of the Higher-Order perfectly matched layer," *Chinese Journal of Computational Physics*, vol. 29, no. 2, pp. 271-276, Mar. 2012.
- [10] N. Okada and J. B. Cole, "Nonstandard finite difference time domain algorithm for Berenger's perfectly matched layer," *Appl. Comp. Electrom. Society (ACES) Journal*, vol. 26, no. 2, pp. 153-159, Feb. 2011.
- [11] J. B. Cole and D. Zhu, "Improved version of the second-order Mur absorbing boundary condition based on a nonstandard finite difference model," *Appl. Comp. Electrom. Society (ACES) Journal*, vol. 24, no. 4, pp. 375-381, August 2009.
- [12] M. Wong and A. R. Sebak, "The floating PML applied to practical FDTD applications," *Appl. Comp. Electrom. Society (ACES) Journal*, vol. 23, no. 2, pp. 110-119, June 2008.
- [13] M. J. Inman, A. Z. Elsherbeni, J. G. Maloney, and B. N. Baker, "Practical implementation of a CPML absorbing boundary for GPU accelerated FDTD technique," *Appl. Comp. Electrom. Society (ACES) Journal*, vol. 23, no. 1, pp. 16-22, March 2008.
- [14] T. Kaufmann, K. Sankaran, C. Fumeaux, and R. Vahldieck, "A review of perfectly matched

absorbers for the finite-volume time-domain method,” *Appl. Comp. Electrom. Society (ACES) Journal*, vol. 23, no. 3, pp. 184-192, Sep. 2008.

- [15] D. M. Sullivan, “Frequency-dependent FDTD methods using Z transforms,” *IEEE Trans. Antennas Propag.*, vol. 40, no. 10, pp. 1223-1230, 1992.
- [16] J. G. Proakis and D. G. Manolakis, *Digital Signal Processing: Principles, Algorithms and Applications*, Prentice Hall International Editions, 3rd Edn., 1996.
- [17] D. F. Kelley and R. J. Luebbers, “Piecewise linear recursive convolution for dispersive media using FDTD,” *IEEE Trans. Antennas Propag.*, vol. 44, no. 6, pp. 792-797, June 1996.
- [18] F. L. Teixeira, W. C. Chew, M. Straka, M. L. Oristaglio, and T. Wang, “Finite-difference time-domain simulation of ground penetrating radar on dispersive, inhomogeneous, and conductive soils,” *IEEE Trans. Geosci. Remote Sens.*, vol. 36, no. 6, pp. 1928-1937, Nov. 1998.
- [19] S. D. Gedney, A. Taflove, and Ed., “The perfectly matched layer absorbing medium,” *Advance in Computational Electrodynamics: The Finite Difference Time Domain*, Boston, MA: Artech House, pp.263-340, 1998.
- [20] O. Montazeri, M. H. Bakr, and Y. M. Haddara, “A PML for electroacoustic waves in piezoelectric materials using FDTD,” *Appl. Comp. Electrom. Society (ACES) Journal*, vol. 26, no. 6, pp. 464-472, June 2011.



Naixing Feng was born in 1987, in Hainan, China. He received the B.Sc. degree in Electronic Science and Technology in 2010, from Tianjin Polytechnic University, Tianjin, China. He is currently pursuing the M.Sc. degree in the School of Electronics and Information Engineering, Tianjin Polytechnic University, Tianjin. His current research interests are in computational electromagnetics and metamaterials.



Jianxiong Li was born in 1969, in Tianjin, China. He received the B.Sc. and M.Sc. degrees in Physics in 1991 and 1994, respectively, and obtained the PhD degree in Communication and Information System in 2007, from Tianjin University, Tianjin, China. His main research interests are in computational electromagnetics, metamaterials, and RFID antenna.



Xiaoming Zhao obtained a PhD degree in textile science from the School of Textiles of Heriot-Watt University (UK) in 2004, and then he continued to his research work in Heriot-Watt University between 2004 and 2010. His work was focused on protective textiles. He joined Tianjin Polytechnic University (China) in 2010, as Professor in Textile Science and Engineering, where he established the Flexible Materials for Protection Research Group.